Biophysical Journal, Volume 99

Supporting Material

Far-Red Fluorescent Protein Excitable with Red Lasers for Flow Cytometry and Super-Resolution STED Nanoscopy

Kateryna S. Morozova,[†] Kiryl D. Piatkevich,[†] Travis J. Gould,[‖] Jinghang Zhang,[‖] Joerg Bewersdorf,[‖] and Vladislav V. Verkhusha[†]

SUPPORTING MATERIAL

```
                    10        20        30        40        50        60
EGFP          MVSKGEELFTGVVPILVELDGDVNGHKFSVSGEGEGDATYGKLTLKFICTTG-KLPVPWPTL
mPlum     MVSKGEENNMAIIKEFMRFKEHMEGSVNGHEFEIEGEGEGRPYEGTQTARLKVTKGGPLPFAWDIL
mRaspberry MVSKGEENNMAIIKEFMRFKVRMEGSVNGHEFEIEGEGEGRPYEGTQTAKLKVTKGGPLPFAWDIL
mKate             MSELIKENMHMKLYMEGTVNNHHFKCTSEGEGKPYEGTQTMRIKVVEGGPLPFAFDIL
mKate2            MSELIKENMHMKLYMEGTVNNHHFKCTSEGEGKPYEGTQTMRIKAVEGGPLPFAFDIL
mNeptune      MVSKGEELIKEDMHMKLYMEGTVNNHHFKCTSEGEGKPYEGTQTGRIKVVEGGPLPFAFDIL
TagRFP657         MSELITENMHMKLYMEGTVNNHHFKCTSEGEGKPYEGTQTQRIKVVEGGPLPFAFDIL

                          70        80        90       100       110       120
EGFP              VTTFTYGVQCFSRYPDHMKQHDFFKSAMPEGYVQERTIFFKDDGNYKTRAEVKFEGDTLV
mPlum             SPQIQYGSKAYVKHPADIP--DYLKLSFPEGFKWERVMNFEDGGVVTVTQDSSLQDGEFI
mRaspberry        SPQCQYGSKGYVKHPADIP--DYLKLSFPEGFKWERVMNFEDGGVVTVTQDSSLQDGEFI
mKate             ATSFMYGSKTFINHTQGIP--DFFKQSFPEGFTWERVTTYEDGGVLTATQDTSLQDGCLI
mKate2            ATSFMYGSKTFINHTQGIP--DFFKQSFPEGFTWERVTTYEDGGVLTATQDTSLQDGCLI
mNeptune          ATCFMYGSKTFINHTQGIP--DFFKQSFPEGFTWERVTTYEDGGVLTATQDTSLQDGCLI
TagRFP657         ATSFMYGSHTFINHTQGIP--DFWKQSFPEGFTWERVTTYEDGGVLTATQDTSLQDGCLI

                         130       140       150       160       170       180
EGFP             NRIELKGIDFKEDGNILGHKLEYNYNSHNVYIMADKQKNGIKVNFKIRHNIEDGSVQLAD
mPlum            YKVKVRGTNFPSDGPVMQKKTMG-WEASTERMYPE--DGALKGEMKMRLRLKDGGHYDAE
mRaspberry       YKVKLRGTNFPSDGPVMQKKTMG-WEASTERMYPE--DGALKGEMKMRLKLKDGGHYDAE
mKate            YNVKIRGVNFPSNGPVMQKKTLG-WEASTEMLYPA--DGGLEGRSDMALKLVGGGHLICN
mKate2           YNVKIRGVNFPSNGPVMQKKTLG-WEASTETLYPA--DGGLEGRADMALKLVGGGHLICN
mNeptune         YNVKIRGVNFPSNGPVMQKKTLG-WEASTETLYPA--DGGLEGRCDMALKLVGGGHLICN
TagRFP657        YNVKIRGVNFPSNGPVMQKKTLG-WEAHTEMLYPA--DGGLEGRTALALKLVGGGHLICN

                         190       200       210       220       230
EGFP             HYQQNTPIGD-GPVLLPDNHYLSTQSALSKDPNEKRDHMVLLEFVTAAGITHGMDELYK
mPlum            VKTTYMAKKP---VQLPGAYKTDIKLDITSH-NEDYTIVEQYERAEGRHSTGGMDELYK
mRaspberry       VKTTYMAKKP---VQLPGAYKTDIKLDITSH-NEDYTIVEQYERAEGRHSTGGMDELYK
mKate            LKTTYRSKKPAKNLKMPGVYYVDRRLERIKE-ADKETYVEQHEVAVARYCDLPSKLGHK
mKate2           LKTTYRSKKPAKNLKMPGVYYVDRRLERIKE-ADKETYVEQHEVAVARYCDLPSKLGHKLN
mNeptune         LKTTYRSKKPAKNLKMPGVYFVDRRLERIKE-ADNETYVEQHEVAVARYCDLPSKLGHKLN
TagRFP657        FKTTYRSKKPAKNLKMPGVYYVDYRLERIKE-ADKETYVEQHEVAVARYCDLPSKLGHKLN
```

FIGURE S1 Alignment of the amino acid sequence of the TagRFP657 protein with EGFP and other monomeric far-red FPs such as mPlum, mRaspberry, mKate, mKate2 and mNeptune. The chromophore forming residues are underlined. Mutations resulting in the conversion of parental mKate into the TagRFP657 protein are highlighted in gray. The alignment numbering follows that for EGFP.

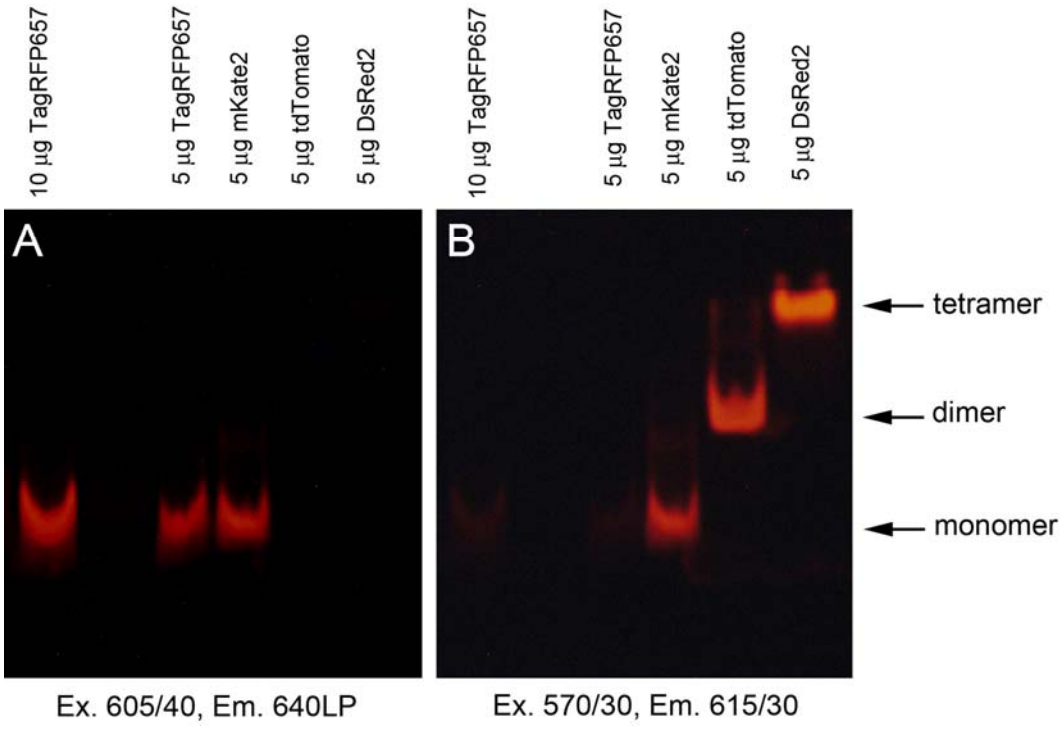

FIGURE S2 Polyacrylamide gel with the purified TagRFP657, mKate2, tdTomato and DsRed2 proteins. The freshly purified proteins were applied in 10 µl aliquots without heating to a 15% polyacrylamide gel containing a low concentration 0.4% SDS. The gels were photographed using a Leica MZ16FL fluorescence stereomicroscope using the far-red (A) and red (B) filter sets (Chroma). mKate2, tdTomato and DsRed2 were used as the monomeric, dimeric and tetrameric native protein standards, respectively. Mobility of the TagRFP657 protein corresponds to its monomeric state even at a high concentration of 1 mg/ml (the left lane in A). Note that TagRFP657 is almost undetectable in the red filter set (B).

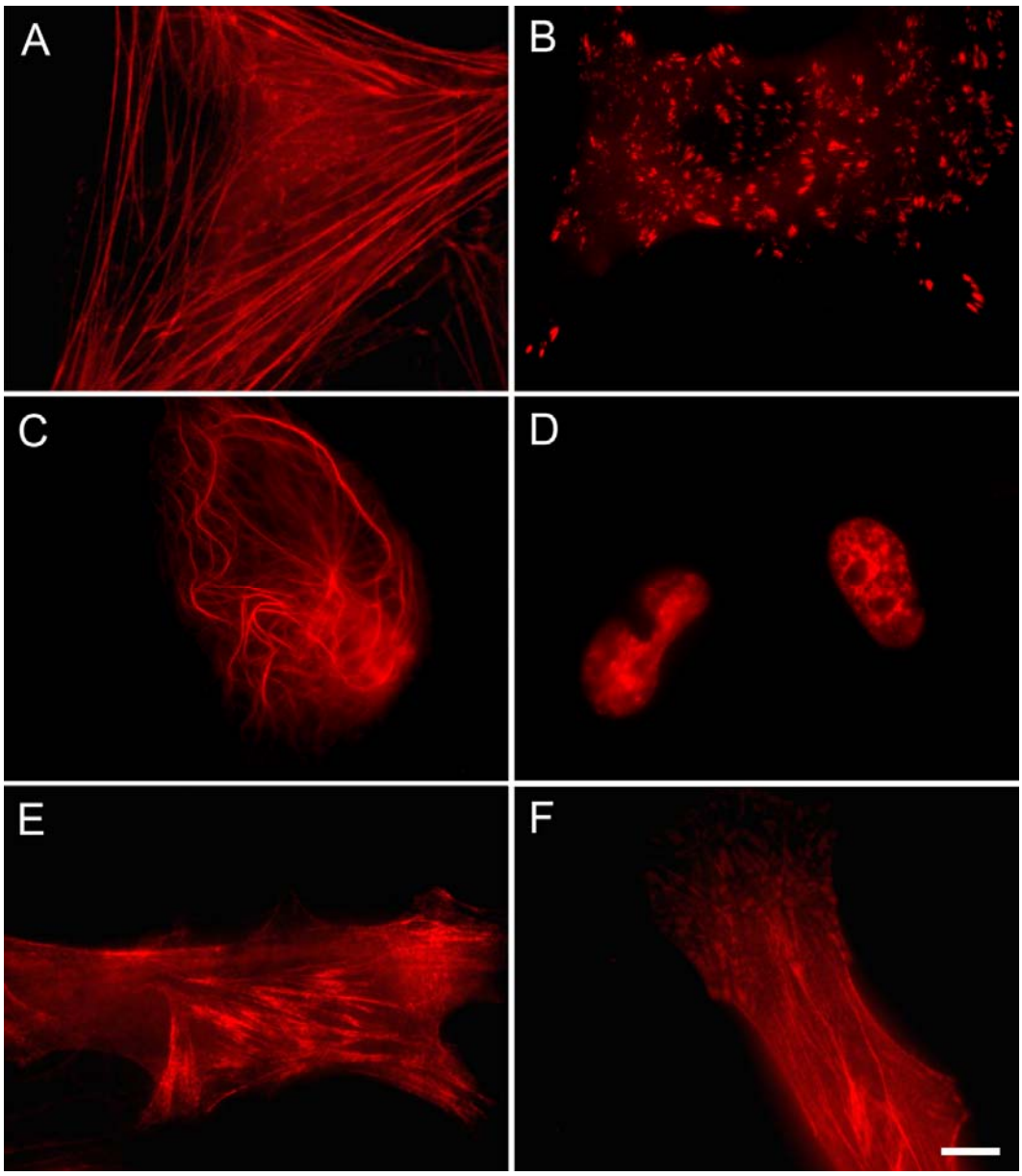

FIGURE S3 Wide-field fluorescence imaging of the TagRFP657 fusion proteins expressed in live HeLa cells. The HeLa cells transfected with (A) TagRFP657-β-actin, (B) paxillin-TagRFP657, (C) microtubule-associating factor EB3-TagRFP657, (D) histone-2B-TagRFP657, (E) myosin-TagRFP657 or (F) α-actinin-TagRFP657 are shown. The images were acquired using an Olympus IX-81 inverted microscope equipped with a 100x 1.4 NA oil objective lens and a far-red filter set (ex. 605/40 nm, em. 640 nm LP). Scale bar is 10 μm.

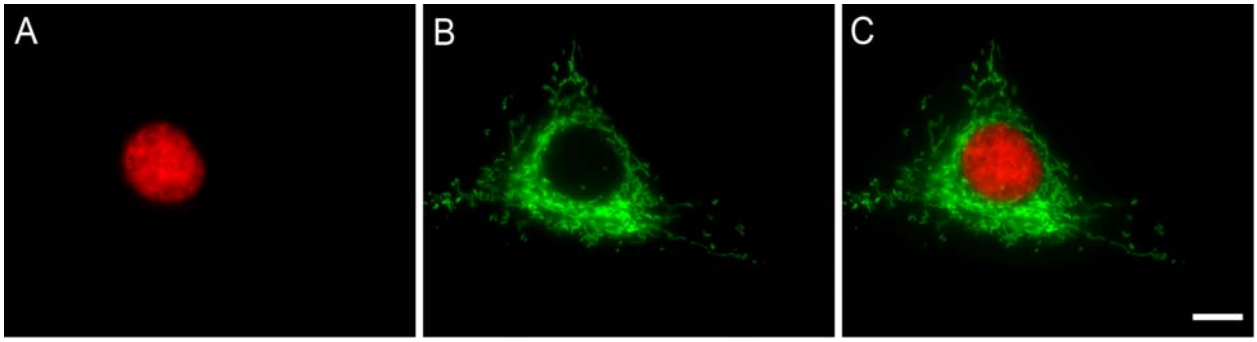

FIGURE S4 Co-expression of histone-2B (H2B) tagged with TagRFP657 and TurboRFP targeted to mitochondria in live HeLa cells. Images of H2B-TagRFP657 are shown in a red (A), TurboRFP-mito in a green pseudocolor (B). Panel (C) shows their overlay. The images were acquired using an Olympus IX-81 inverted microscope equipped with a 100x 1.4 NA oil objective lens, and near-red (ex. 540/20 nm, em. 575/30 nm) and far-red (ex. 605/40 nm, em. 640 nm LP) filter sets. Scale bar is 10 μm.

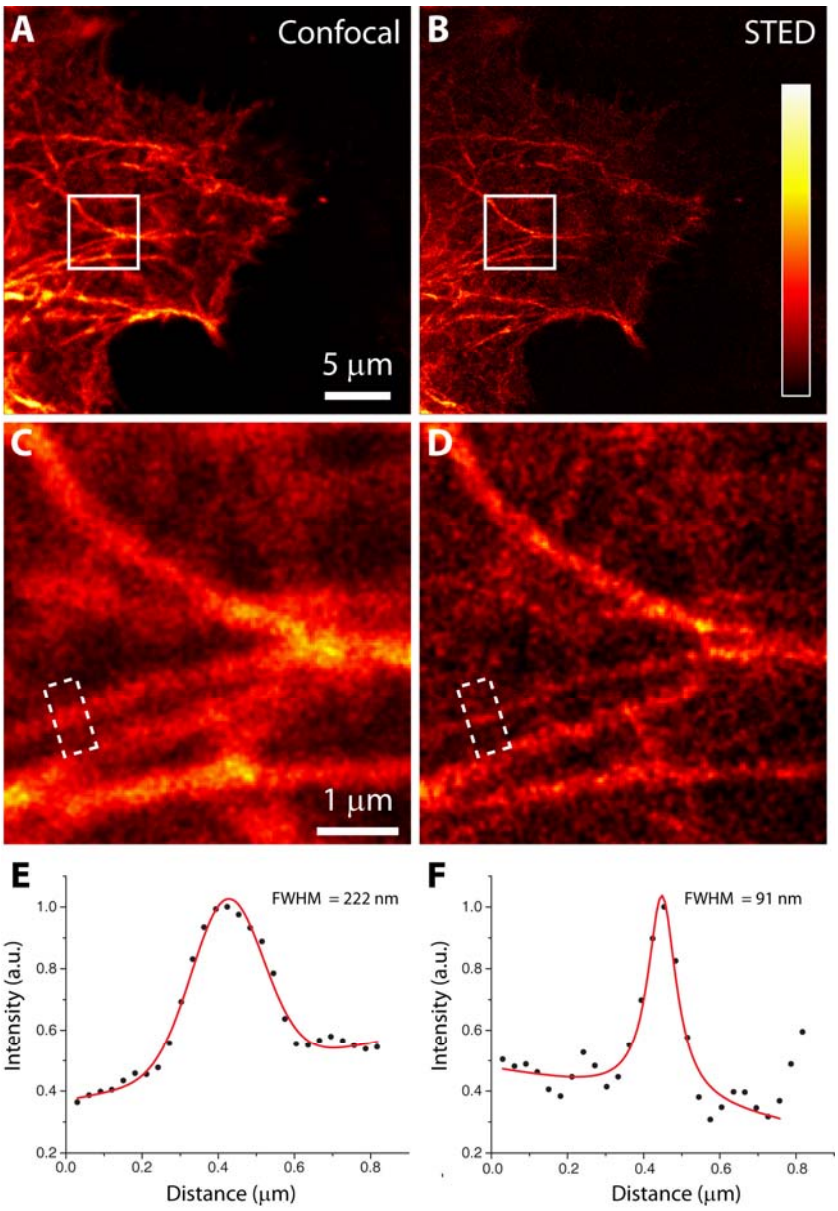

FIGURE S5 Imaging of α-actinin-TagRFP657 fusion in fixed HeLa cells using (A) standard confocal and (B) super-resolution STED microscopy. Magnified views of the square areas in (A, B) are shown for confocal (C) and STED (D) images. Profiles displayed in (E) and (F) were generated from identical regions of interest (ROIs) shown in (C, D). The profiles were measured along the longer side of the ROIs, averaging over the shorter side. Solid red lines in (E) and (F) indicate the Gaussian (confocal) and Lorentzian (STED) fits used to determine the displayed FWHM values. Due to thickness of the actin bundles, the observed structures appear thicker than the resolution limit of the instrument. Image color-maps were scaled to minimum and maximum values in (A, B).

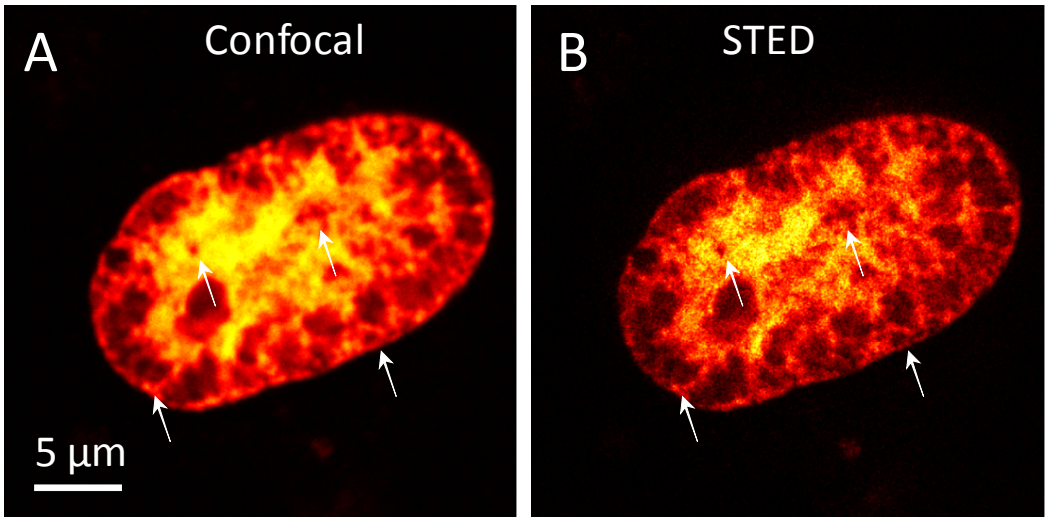

FIGURE S6 Imaging of histone-2B-TagRFP657 fusion in fixed HeLa cells using (A) standard confocal and (B) super-resolution STED microscopy. H2B is present at high density throughout the nucleus. While no prominent structures between the Leica TCS STED resolution limit of ~70 nm and conventional confocal resolution limit (>200 nm) are apparent, STED significantly improves the contrast of the observed chromatin heterogeneity on the intermediate length scales, as indicated with the white arrows.

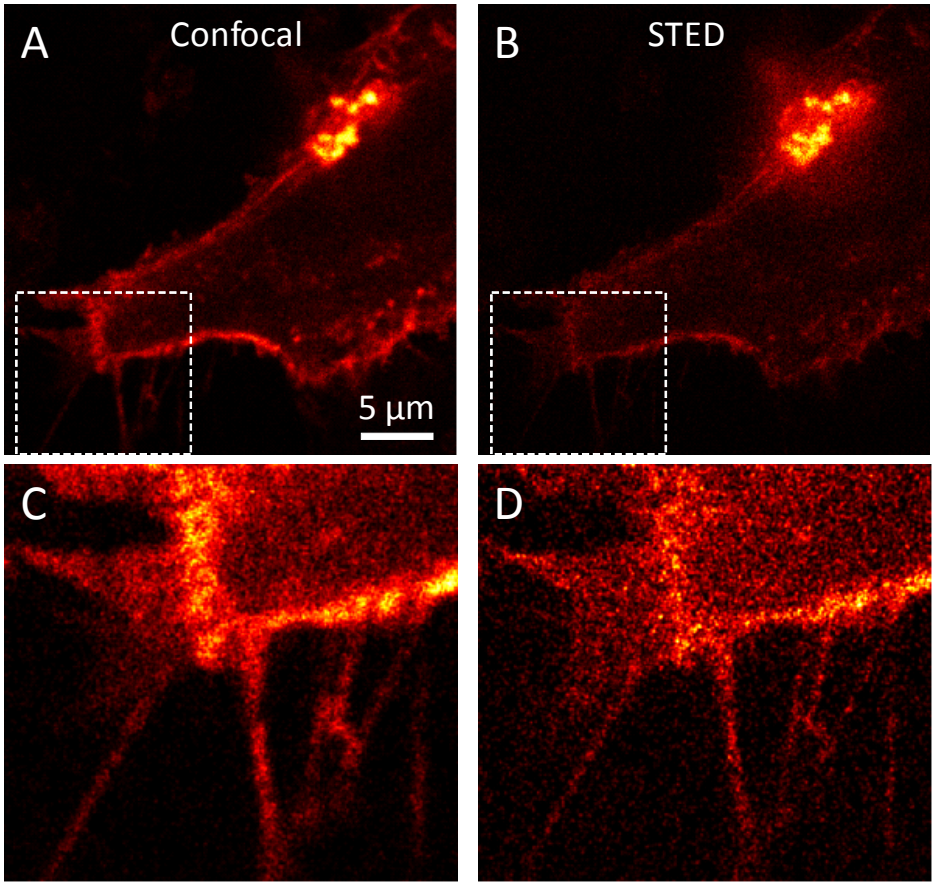

FIGURE S7 Imaging of EGFR-TagRFP657 fusion in fixed HeLa cells using (A) standard confocal and (B) super-resolution STED microscopy. The area marked by the white boxes (A, B) is magnified in (C, D). STED microscopy reveals the fine details of filopodia at the edge of the cell (D), which are barely detected in the confocal image (C).

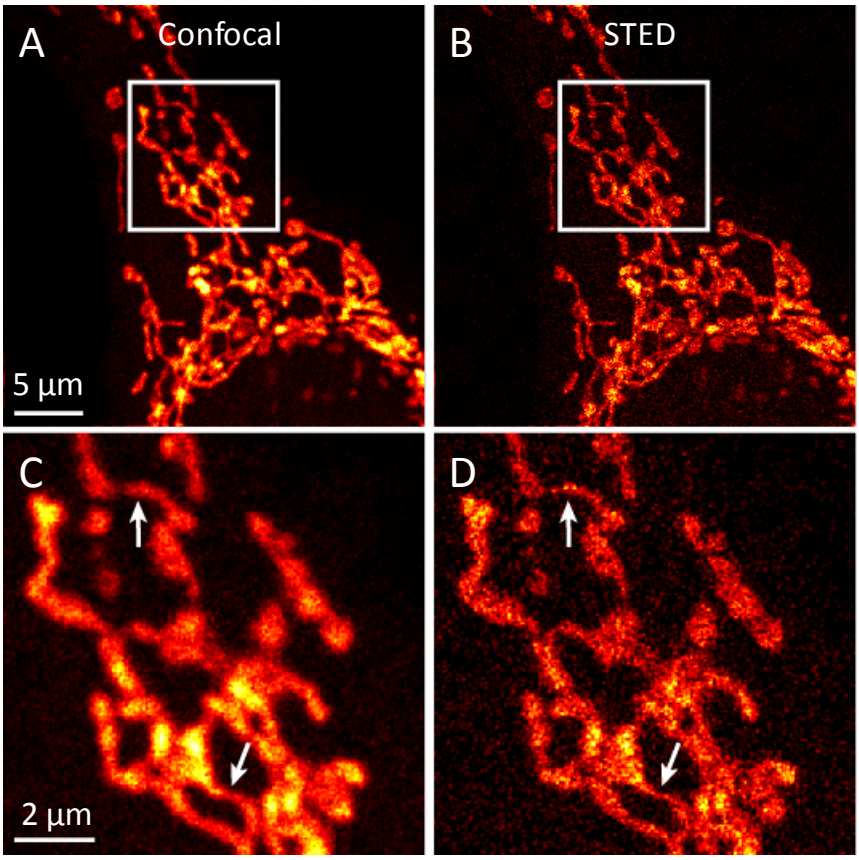

FIGURE S8 Imaging of TagRFP657 fused to mitochondria targeting sequence (human cytochrome C oxidase subunit VIII) in fixed HeLa cells using standard confocal (A) and super-resolution STED microscopy (B). White boxes (A, B) are magnified in (C, D). The large diameter of mitochondria (typically >250 nm) is still represented in the super-resolution images demonstrating that the image enhancement observed in the other STED images is object-dependent and not an instrument or image processing artifact. White arrows point out a few examples of unusually thin tubules (D), a feature only hinted at by the low observed intensity in the corresponding regions in the confocal images (C).

MATERIAL AND METHODS

Mutagenesis and screening of bacterial libraries.

A gene encoding the far-red fluorescent protein mKate (1) was PCR (polymerase chain reaction) amplified as a *BamH*I-*Hind*III fragment and inserted into the *Bgl*II-*Hind*III sites of the pBAD/His-B vector (Invitrogen). Site specific mutagenesis was performed using a QuikChange Site-Directed Mutagenesis Kit (Stratagene). For simultaneous mutagenesis at several positions, including a site-specific saturated mutagenesis (i.e., all 20 amino acids were encoded using the mixture of primers), the overlap-extension approach has been applied (2). Random mutagenesis was performed with a GeneMorph II Random Mutagenesis Kit (Stratagene) using conditions that resulted in a mutation frequency of up to 16 mutations per 1000 base pairs. After the mutagenesis a mixture of the mutants was electroporated into LMG194 host cells (Invitrogen).

Typical mutant libraries for each screen with fluorescence-activated cell sorter (FACS) consisted of about 10^7 independent clones. LMG194 cells were grown at 37^0C overnight in RM minimal medium supplemented with ampicillin. Protein expression in the libraries was induced overnight at 37^0C with 0.002% arabinose. The following morning, the expressing bacteria were washed with phosphate buffered saline (PBS) and then diluted with PBS to an optical density of 0.02 at 600 nm for FACS sorting. FACS screening of several first mutant libraries was performed with a MoFlo XDP cell sorter (Beckman Coulter) equipped with the standard Ar and Kr gas lasers, and a 592 nm 300 mW fiber laser (VFL-P-300-592, MPB Communications). A FACSAria II cell sorter (Becton Dickinson) equipped with 407 nm, 488 nm, 561 nm and 638 nm solid-state lasers was used to screen for red-shifted mutants in later libraries. Typically, about 10 sizes of each library were sorted for positive selection using FACS either with the 568 nm Kr line and 592 nm fiber laser (MoFlo XDP), or with 561 nm and 638 nm solid-state lasers (FACSAria II), and with the 630/30 and 670/30 nm emission filters, respectively. Bacterial cells with the greatest far-red to red ratio and the brightest in far-red channel were collected with both FACS instruments.

The collected were rescued in rich SOC medium at 37°C for one hour, and then plated on Petri dishes with 0.02% arabinose. The next day, colonies were analyzed using the far-red to red fluorescence ratio with a Leica MZ16F fluorescence stereomicroscope equipped with red (ex. 570/30 nm, em. 615/40 nm) and far-red (ex. 605/40 nm, em. 640 nm LP) filter sets (Chroma). For further analysis, the 20-30 brightest in far-red clones were selected and applied for

sequencing. A mixture of 2-5 selected variants was then used as a template for the next round of mutagenesis.

Protein purification and characterization.

mKate (1) and its mutants with polyhistidine tags were expressed in LMG194 bacterial cells grown in RM medium supplemented with 0.002% arabinose overnight at 37^0C and then purified using a Ni-NTA agarose (Qiagen). The excitation and emission spectra were measured using a FluoroMax-3 spectrofluorometer (Jobin Yvon). For absorbance measurements a Hitachi U-3010 spectrophotometer was used.

To determine extinction coefficients, we relied on measuring mature chromophore concentrations. For that purpose, the purified fluorescence proteins were alkali-denatured. It is known that the extinction coefficient of the synthetic compound of the tyrosine-containing GFP-like chromophores is 44,000 $M^{-1}cm^{-1}$ at 447 nm in 1 M NaOH (3). Based on the absorbance of the native and denatured proteins, molar extinction coefficients for the native states were calculated. The concentration of proteins was determined using the BCA Protein Assay Kit (Pierce). For determination of the quantum yields, fluorescence of TagRFP657 was compared with equally absorbing mKate2 (quantum yield is 0.40 (4)). pH titrations were performed using a series of buffers (100 mM NaOAc, 300 mM NaCl for pH 2.5-5.0, and 100 mM NaH_2PO_4, 300 mM NaCl for pH 4.5-9.0).

To study protein maturation, LMG194 bacterial cells were grown at 37^0C overnight in RM medium supplemented with ampicillin. The following morning, cells were diluted to optical density 1.0 at 600 nm, and 0.2% arabinose was added. Upon induction of protein expression the bacterial cultures were grown at 37^0C in 50 ml tubes filled to the brim and tightly sealed to restrict oxygen availability. After 1 hour, the cultures were centrifuged in the same tightly closed tubes. After opening the tubes, the fluorescent proteins were purified using the Ni-NTA resin (Qiagen) within 30-40 min with all procedures and buffers at or below 4^0C. Protein maturation was performed at 37^0C in PBS pH 7.5 using the FluoroMax-3 spectrofluorometer.

Photobleaching measurements were performed using bacterial streaks expressing FPs covered with glass coverslips using an Olympus IX81 inverted microscope equipped with a 200 W metal halide lamp (Prior), a 100x 1.4 NA oil immersion lens (UPlanSApo, Olympus) and a 605/40 nm filter (Chroma). The bacterial streaks were photobleached at different light intensities, measured at the back focal plane of the objective lens using a PM100 power meter (ThorLabs).

The photobleaching curves were then normalized to the spectral output of the metal halide lamp, transmission profile of the excitation filter and dichroic mirror, absorbance spectra of the proteins.

Plasmids for mammalian cells.

To construct a pTagRFP657-C1 vector, the TagRFP657 gene was PCR amplified as a NheI-BglII fragment and swapped with the EGFP gene in a pEGFP-C1 vector (Clontech). To construct a pTagRFP657-N1 vector, the TagRFP657 gene was PCR amplified as a *Age*I-*Not*I fragment and swapped with the EGFP gene in a pEGFP-N1 vector (Clontech). To generate vectors encoding fusion constructs, the appropriate cloning vector and the respective mTagBFP (5) fusion vector were digested with specific enzymes and ligated together after gel purification. Thus, to prepare TagRFP657 N-terminal fusions, the following digests were performed: human α-actinin with *Eco*RI and *Not*I, human histone-2B with *BamH*I and *Not*I, chicken paxillin with *BamH*I and *Not*I, human myosin with *BamH*I and *Not*I, human microtubule-associated factor EB3 with *BamH*I and *Not*I, and human cytochrome C oxidase subunit VIII (for targeting to mitochondria) with *BamH*I and *Not*I (mTagBFP fusion vectors were kindly provided by M. Davidson, Florida State University). To prepare a pTagRFP657-β-actin plasmid, the TagRFP657 gene was PCR amplified as a *Nhe*I-*Bgl*II fragment and swapped with the EGFP gene in the pEGFP-β-actin plasmid (Clontech). To construct a pEGFR-TagRFP657 plasmid encoding elongation growth factor receptor tagged with TagRFP657, a *Sac*II-*Bsr*GI fragment containing the TagRFP657 gene was cut out from the pTagRFP657-N1 vector and swapped with the mRFP1 gene in the pEGFR-mRFP1 plasmid (6). To make a pTfR-TagRFP657 plasmid encoding transferrin receptor tagged with TagRFP657, a PCR-amplified *Bam*HI-*Not*I fragment encoding the TagRFP657 gene was swapped with the mCherry gene in the pTfR-mCherry plasmid (7). The pmKate-N1 (1), pTagRFP-N1 (8) and pTurboRFP-mito (8) plasmids were kindly provided by D.Chudakov and K.Lukyanov (Institute of Bioorganic Chemistry, Moscow, Russia).

Mammalian cell culture and transfection.

HeLa cells were cultured in DMEM medium with 10% FBS and 0.5% penicillin-streptomycin (all from Invitrogen). Transfections were performed with indicated above plasmids using an Effectene reagent (Qiagen) as per manufacturer's protocol. HeLa cells were seeded on 25 mm glass coverslips in a 6-well plate so they would be 40% confluence the following day. The pre-

incubated mixture of 0.4 μg DNA with Effectene and supplementary reagents was added to the cells. After 24 hours, the growth media with Effectene-DNA complexes was replaced by fresh one.

Widefield microscopy and flow cytometry of cells.

Imaging of HeLa cells was performed 48-72 h after the transfection. Cells were imaged using an Olympus IX81 inverted microscope equipped with 200W metal halide lamp, a 100x 1.4 NA oil objective lens (UPlanSApo, Olympus), near-red (ex. 540/20 nm, em. 575/30 nm), red (ex. 570/30 nm, em. 615/30 nm), and far-red (ex. 605/40 nm, em. 640 nm LP) filter sets (Chroma), and operated with a SlideBook v.4.1 software (Intelligent Imaging Innovations). Flow cytometry detection of the TagRFP657, mKate (1) and TagRFP (8) expressing cells was performed using the FACSAria II cell sorter described above.

STED microscopy of mammalian cells.

For STED imaging, HeLa cells transfected with TagRFP657 fusions were fixed using 4% paraformaldehyde and mounted on glass slides using Mowiol 4-88 (Calbiochem). No antibleaching additives were used. Samples were imaged using a commercial Leica TCS STED microscope equipped with a 640 nm diode laser (PDL 800-B, PicoQuant) for excitation (~180-225 μW) and a tunable Ti:Sapphire laser (Mai Tai, Spectra Physics) set to 750 nm for depletion (~142 mW). Laser powers were measured at the objective back aperture. Fluorescence from the samples was collected by a 100x 1.4 NA oil immersion objective lens (HcxPlApo STED, Leica), filtered by two bandpass filters (FF01-685/40, Semrock), and detected by an avalanche photodiode. The pinhole was set to 0.7 Airy units and the pixel size was 30.3 nm. Images of 1024 x 1024 pixels were acquired at a scan speed of 1000 lines per second. Confocal images were taken sequentially after the STED images and differ in settings only by the number of line averages performed (16 for STED, 6 for confocal). Images were later smoothed by a two-dimensional Gaussian with a full-width half-maxima (FWHM) of 2 pixels using an ImSpector software (Andreas Schoenle, Max-Planck Institute for Biophysical Chemistry, Germany). Line profiles were generated by averaging across the 12 pixel wide region of interests indicated by the white boxes shown in Figs. 3C,D and S5C,D. Using Origin v.8.0 (OriginLab) software, line profiles were fitted to determine FWHM using either one-dimensional Gaussian (confocal) or Lorentzian (STED) plus a linear background term and constant offset.

REFERENCES

1. Shcherbo, D., E. M. Merzlyak, T. V. Chepurnykh, A. F. Fradkov, G. V. Ermakova, E. A. Solovieva, K. A. Lukyanov, E. A. Bogdanova, A. G. Zaraisky, S. Lukyanov, and D. A. Chudakov. 2007. Bright far-red fluorescent protein for whole-body imaging. *Nat. Methods*. 4:741-746.
2. Ho, S. N., H. D. Hunt, R. M. Horton, J. K. Pullen, and L. R. Pease. 1989. Site-directed mutagenesis by overlap extension using the polymerase chain reaction. *Gene.* 77:51-59.
3. Chudakov, D. M., V. V. Verkhusha, D. B. Staroverov, S. Lukyanov, and K. A. Lukyanov. 2004. Photoswitchable cyan fluorescent protein for protein tracking. *Nat. Biotechnol.* 22:1435-1439.
4. Shcherbo, D., C. S. Murphy, T. V. Chepurnykh, A. S. Shcheglov, V. V. Verkhusha, V. Z. Pletnev, K. L. Hazelwood, S. Lukyanov, M. W. Davidson, and D. M. Chudakov. 2009. Far-red fluorescent tags for protein imaging in living tissues. *Biochem. J.* 418:567-574.
5. Subach, O. M., I. S. Gundorov, M. Yoshimura, F. V. Subach, J. Zhang, G. Gruenwald, E. A. Souslova, D. M. Chudakov, and V. V. Verkhusha. 2008. Conversion of red fluorescent protein into a bright blue probe. *Chem. Biol.* 15:1116-1124.
6. Galperin, E., Verkhusha, V. V., and Sorkin, A. 2004. Three-chromophore FRET microscopy to analyze multiprotein interactions in living cells. *Nat. Methods.* 1:209-217.
7. Subach, F. V., Patterson, G. H., Manley, S., Gillette, J. M., Lippincott-Schwartz, J., and Verkhusha, V. V. 2009. Photoactivatable mCherry for high-resolution two-color fluorescence microscopy. *Nat. Methods.* 6:153-159.
8. Merzlyak, E. M., J. Goedhart, D. Shcherbo, M. E. Bulina, A. S. Scheglov, A. F. Fradkov, A. Gaintzeva, K. A. Lukyanov, S. Lukyaniov, T. W. J. Gadella, and D. M. Chudakov. 2007. Bright monomeric red fluorescent protein with an extended fluorescence lifetime. *Nat. Methods.* 4:555-557.